HHS Public Access

Author manuscript

Neuropsychologia. Author manuscript; available in PMC 2018 May 01.

Published in final edited form as:

Neuropsychologia. 2017 May ; 99: 37–47. doi:10.1016/j.neuropsychologia.2017.02.016.

Focused stimulation of dorsal subthalamic nucleus improves reactive inhibitory control of action impulses

N.C. van Wouwe[a,*], **S. Pallavaram**[c], **F.T. Phibbs**[a], **D. Martinez-Ramirez**[d], **J.S. Neimat**[b], **B.M. Dawant**[c], **P.F. D'Haese**[c], **K.E. Kanoff**[a], **W.P.M. van den Wildenberg**[e], **M.S. Okun**[d], and **S.A. Wylie**[b]

[a]Department of Neurology, Vanderbilt University Medical Center, Nashville, TN, USA [b]Department of Neurosurgery, University of Louisville Medical Center, Louisville, KY, USA [c]Department of Engineering, Vanderbilt University, Nashville, TN, USA [d]Department of Neurology, University of Florida Medical Center, Gainesville, Florida, USA [e]Cognitive Science Center Amsterdam and Psychology Department, University of Amsterdam, Amsterdam, The Netherlands

Abstract

Frontal-basal ganglia circuitry dysfunction caused by Parkinson's disease impairs important executive cognitive processes, such as the ability to inhibit impulsive action tendencies. Subthalamic Nucleus Deep Brain Stimulation in Parkinson's disease improves the reactive inhibition of impulsive actions that interfere with goal-directed behavior. An unresolved question is whether this effect depends on stimulation of a particular Subthalamic Nucleus subregion. The current study aimed to 1) replicate previous findings and additionally investigate the effect of chronic versus acute Subthalamic Nucleus stimulation on inhibitory control in Parkinson's disease patients off dopaminergic medication 2) test whether stimulating Subthalamic Nucleus subregions differentially modulate proactive response control and the proficiency of reactive inhibitory control. In the first experiment, twelve Parkinson's disease patients completed three sessions of the Simon task, Off Deep brain stimulation and medication, on acute Deep Brain Stimulation and on chronic Deep Brain Stimulation. Experiment 2 consisted of 11 Parkinson's disease patients with Subthalamic Nucleus Deep Brain Stimulation (off medication) who completed two testing sessions involving of a Simon task either with stimulation of the dorsal or the ventral contact in the Subthalamic Nucleus. Our findings show that Deep Brain Stimulation improves reactive inhibitory control, regardless of medication and regardless of whether it concerns chronic or acute Subthalamic Nucleus stimulation. More importantly, selective stimulation of dorsal and ventral subregions of the Subthalamic Nucleus indicates that especially the dorsal Subthalamic Nucleus circuitries are crucial for modulating the reactive inhibitory control of motor actions.

[*]Correspondence to: Medical Center North Department of Neurology, Vanderbilt University Medical Center, 1161 21st Avenue South, A-0118, Nashville, TN 37232, USA. nelleke.van.wouwe@vanderbilt.edu (N.C. van Wouwe).

Disclosure statements

Dr. Dawant and Dr. D'Haese are founders and equity holders in Neurotargeting, LLC., that licenses some of the technology from Vanderbilt University described in this article. Dr. Pallavaram is also an equity holder in Neurotargeting, LLC. Dr. Phibbs has done consulting for Boston Scientific, Medtronic and Teva. There are no other conflicts of interest to report.

Keywords

Parkinson's disease; Simon task; Inhibititory control; Subthalamic nucleus deep brain stimulation; Subthalamic nucleus subregions

1. Introduction

The potential dissociation of functional subterritories within the STN has generated considerable clinical interest and sparked debate. Clinically, the ability to direct high-frequency electrical stimulation to targeted STN substructures holds promise as a flexible intervention to simultaneously treat a wider range of motor, cognitive, and emotional deficits that emerge in Parkinson's disease. The debate centers on the notion of functional subdivisions in the STN. Some anatomical and connectivity studies suggest that the distribution of prefrontal inputs to STN maintains topographical segregation along the dorsolateral to ventromedial STN axis that follows, respectively, a motor (e.g., primary motor, pre-motor, supplementary motor) to cognitive (e.g., dorsolateral prefrontal cortex) to limbic (e.g., orbitofrontal cortex) gradient (Haynes and Haber, 2013). Others have questioned the fidelity of topographically defined STN subregions by pointing to the diffuse overlap of prefrontal inputs across the STN structure (Keuken et al., 2012). Contributing to this debate are a limited set of pioneering studies in Parkinson's disease that tested the functional architecture of STN substructures by contrasting behavioral effects of stimulating electrode contacts situated relatively more dorsal or more ventral along the lead wire targeting STN (Greenhouse et al., 2011, 2013; Hershey et al., 2010). While these studies have disclosed dissociable behavioral effects along the dorsal-ventral axis, most have been restricted by the confounding influence of dopaminergic medications in Parkinson's disease, use of electrodes and stimulation parameters chosen clinically for motor symptom control that inevitably produce large fields of tissue activation, and limited specification of electrode positioning, including electrodes often positioned outside of the STN.

The goal of this investigation was to address some of these limitations while testing the hypothesis that stimulating dorsal and ventral STN substructures produces dissociable effects on two critical components of executive cognitive control, *proactive impulse control* and *reactive inhibitory control*. These forms of cognitive control are separable experimentally and have been linked to frontal-basal ganglia circuitries (Aron et al., 2007; Forstmann et al., 2008a, b, c; Jahfari et al., 2011; Gillan et al., 2011; Holl et al., 2013; van den Wildenberg et al., 2010; Worbe et al., 2011). Studies show their compromise in Parkinson's disease and their modulation by dopamine pharmacotherapy (Wylie et al., 2009a, b, 2010a, b, 2012a, b, 2013). These control mechanisms are crucial for navigating dynamic, action-oriented environments that may trigger conflicting, undesired, or impulsive response tendencies. A *proactive impulse control* mechanism provides a first line of defense against strong motor impulses by governing the motor system's global susceptibility to acting on initial response impulses. Poor *proactive impulse control* leads to higher rates of fast, impulsive action errors in conflict situations. Even when impulsive responses activated in the motor system fail to trigger an overt response error, they directly interfere with the speed of selecting a desired action. In this situation, a *reactive inhibitory control* mechanism

is engaged to suppress the interference from the activated response impulse (Aron and Poldrack, 2006; Ballanger et al., 2009; Botvinick et al., 2001; Cavanagh et al., 2012; Forstmann et al., 2008a, b, c; Frank, 2006; Mansfield et al., 2011; Ridderinkhof et al., 2004; Wylie et al., 2010a, b; Zaghloul et al., 2012).

The STN has been postulated as a key node in both cognitive control circuitries, and data point to STN involvement when making proactive adjustments in response and decision thresholds as well as in situations eliciting reactive inhibitory control (Frank et al., 2006, 2007; Kolomiets et al., 2001; Nambu et al., 2002; Wylie et al., 2010a, b). Human Parkinson's disease studies investigating the effects of STN DBS using clinically-determined electrodes and stimulation parameters and studies of STN-lesioned animals frequently report an increase in fast, premature response errors, suggesting that *proactive impulse control* may be lowered or disrupted (Eagle and Baunez, 2010; Frank et al., 2006, 2007; Campbell et al., 2008; Ballanger et al., 2009; Hershey et al., 2004; Jahanshahi et al., 2000; Witt et al., 2004). Moreover, Hershey et al. (2010) suggested that stimulating the STN through a more ventrally situated electrode contact using clinical stimulation parameters induced an increase in impulsive commission errors in a go/no-go task. STN DBS applied using clinically-derived stimulation parameters also appears to modulate *reactive inhibitory control* mechanisms engaged to inhibit activated but undesired actions (van den Wildenberg et al., 2006; Wylie et al., 2010a, b; Swann et al., 2011; Mirabella et al., 2012). In a prior study of dopamine-medicated Parkinson's patients, we reported that STN DBS using clinical parameters produced both patterns of effects by inducing greater susceptibility to acting on strong initial impulses (i.e., poorer *proactive impulse control*), but conversely improving the proficiency of *reactive inhibitory control* engaged to suppress interference from these impulses (Wylie et al., 2010a, b).

In the current investigation, we conducted two critical follow-up experiments. The first involved a replication of STN DBS effects (using clinically-defined electrode and stimulation parameters) on *proactive impulse control* and *reactive inhibitory control* that we reported previously, but this time patients performed withdrawn from their dopaminergic medications. In the second experiment, we tested the dissociable effects of stimulating in dorsal versus ventral STN on *proactive impulse control* and *reactive inhibitory control*. We recruited a new sample of PD patients withdrawn from dopaminergic medications and mapped their bilateral DBS contacts *a priori* to dorsal and ventral STN subregions to ensure electrode contacts were embedded within (or intersecting) the STN structure. We then applied more focused stimulation parameters to restrict the projected field of tissue activation to the dorsal or to the ventral STN subregion in separate testing sessions. Given our finding that clinically-determined DBS, which typically utilizes contacts situated more dorsally along the electrode lead and STN, improves reactive inhibitory control, we predicted that the improvement in the proficiency of inhibitory control would be greatest when stimulating a relatively dorsal STN subregion compared to a relatively ventral STN subregion. Confirmation of this pattern would provide new evidence that dorsal STN circuitries play a direct role in reactive inhibitory motor control processes. Given a suggested link between impulsive errors and stimulation of a relatively ventral STN contacts reported by Hershey et al. (2010), we predicted that stimulating a ventral STN subregion might lead to poorer *proactive impulse control* revealed by higher rates of fast impulsive errors.

2. Experiment 1

2.1. Methods

2.1.1. Participants—Parkinson's disease participants (n =12) were recruited from the Movement Disorders Clinic at Vanderbilt University Medical Center, and healthy controls (n=22) were recruited from community advertisement or as qualifying family members of Parkinson's disease participants. All participants met the following exclusion criteria: no history of (i) neurological condition (besides Parkinson's Disease); (ii) bipolar affective disorder, schizophrenia, or other psychiatric condition known to compromise executive cognitive functions; or (iii) severe mood disorder determined by questionnaire and interview; or (iv) medical condition known to interfere with cognition (e.g., diabetes, heart condition, pulmonary disease). Parkinson's disease.

patients were treated with bilateral STN DBS (Activa PC Medtronic neurostimulator, Medtronic Inc., Minneapolis, Minnesota) for at least 6 months and exhibited a clinically effective and stable response to it. The surgical procedure for STN DBS utilized standard stereotactic techniques with microelectrode recordings for electrophysiological localization reported previously (Konrad et al., 2011). All patients were prescribed dopaminergic medications, but completed cognitive performance in an OFF state after withdrawing from their dopaminergic medications (levodopa > 24 h; agonist > 48 h). Parkinson's disease motor symptoms were graded using the Unified Parkinson's Disease Rating Scale III motor subscore across stimulation states. Dopamine medication dosages were converted to levodopa equivalent daily dose (LEDD) values (Weintraub et al., 2006).

All Parkinson's disease patients performed at a level on the Mini-Mental Status Examination (MMSE; Folstein et al., 1975) or Dementia Rating Scale 2 (DRS-2, Jurica & Leitten, 2001) that ruled out dementia but permitted very mild to minimal gross cognitive difficulties (MMSE scores ≥25, DRS-2 scores > 129). Healthy controls all scored greater than a 26 on the MMSE (mean =29.4, std error =.19). All participants reported stable mood functioning and the absence of major depression during a clinical interview, but we allowed endorsements of mild to low moderate symptoms of depression on the Center for Epidemiological Studies Depression (Radloff, 1977) questionnaire or Beck Depression Inventory (Beck et al., 1961). All participants had corrected-to-normal vision. They all provided informed consent prior in full compliance with the standards of ethical conduct in human investigation as regulated by Vanderbilt University.

2.1.2. Experimental task and procedures—We administered the Simon task and applied the Dual-Process Activation-Suppression conceptual-analytic framework to isolate measures of *proactive impulse control* and *reactive inhibitory control* (Ridderinkhof, 2002; van den Wildenberg et al., 2010). In our computerized version of the Simon task, participants make speeded reactions based on the color of a circle that appears to the left or to the right of a central fixation point. When a circle appears in a particular visual half-field, an impulse to respond with the hand to the same side is activated automatically. If the color of the circle also calls for a response with that same hand, reactions are both fast and highly accurate. However, if the automatic impulse is opposite the hand signaled by the circle's color, conflict is produced leading to higher rates of fast, impulsive errors and heightened

interference with the speed of issuing the correct response. A detailed description of our task stimuli and parameters can be found elsewhere (Wylie et al., 2010a, b). Briefly, participants used handheld response grips to register left or right thumb button presses to a series of blue or green colored circles that appeared one at a time to the left or to the right of a central fixation point on the screen. Participants were instructed to respond to the color of the circle based on a predetermined mapping between the color of the circle and a response hand (e.g., green circle=right-thumb press; blue circle=left-thumb press). The mappings between colors and response hands were counterbalanced across participants, but preserved across testing sessions within individuals. A circle remained on the screen until a response was issued or 1200 ms elapsed, either of which triggered the onset of the next trial.

Participants were encouraged to respond as quickly and as accurately as possible to the circle when it appeared. To elicit the Simon effect, two trial types manipulated the correspondence between the spatial location of the circle (i.e., to the left or to the right of fixation) and the response signaled by its color. For *Corresponding* trials, the circle appeared to the side of fixation that matched the response side signaled by the color of the stimulus (e.g., a green circle calling for a right-hand response appeared to the right side of fixation). For *Non-corresponding* trials, the circle appeared on the side of fixation opposite the side of the response signaled by the circle's color (e.g., a green circle calling for a right-hand response appeared on the left side of fixation). Cs and Nc trial types were presented randomly, but with equal probability, within each block of trials. Across both experiments, participants completed 60 practice trials followed by 240 experimental trials (i.e., 4 blocks of 60 trials) equally divided among Cs and Nc trial types.

HC participants completed one session of the Simon task. Parkinson's disease participants completed three sessions of the task corresponding to different DBS states. All patients arrived to the experimental study in a dopamine medication withdrawn state but with DBS turned on using optimal clinical parameters (Table 2). In a first session, patients completed a block of practice trials, and then performed the task without any interruption or changes to their DBS settings, which we will refer to as the *chronic DBS* condition. After the cognitive testing, the UPDRS was administered. Next, the DBS device was completely turned off for 30 min. Previous work suggests that this time period accounts for the majority of changes in motor response and is sufficient to find effects on inhibitory control (Temperli et al., 2003; Lopiano et al., 2003; Waldau et al., 2011; Wylie et al., 2010a, b). Patients were then assigned, in a counterbalanced manner, to either an *off DBS* session or to an *acute DBS* session, with the latter representing resumption of clinically optimized DBS but after DBS had been interrupted and turned off. Before starting experimental testing in the acute DBS session, a 30-min wait period was implemented subsequent to turning on the stimulation. The purpose of this design was to rule out differences that might be attributable to interrupted versus uninterrupted DBS effects, that is inevitable in designs counterbalancing on versus off DBS conditions. Our design attempts to ensure that any experimental effects are not solely attributable to an interruption of DBS confound. All three sessions were completed on the same day with rest breaks provided between sessions.

2.1.3. Statistical techniques—Reaction time latencies for Cs and Nc trials faster than 180 ms (i.e., anticipatory reactions) and slower than 3 standard deviations of the mean

within each condition and judged as clear outliers following visual inspection were excluded, but accounted for fewer than 1% of trials across participants (see Wylie et al., 2010a). Mean RT and square-root transformed accuracy rates were computed for each level of *Correspondence* to analyze mean Simon interference costs on RT and on accuracy.

As reported previously (Wylie et al., 2010a, b), the DPAS model provided the conceptual and analytical framework to uncover the temporal dynamics of response activation and suppression by means of distributional analyses. Global RT measures and even mean interference effects are often non-disclosing of specific cognitive control demands (Mirabella et al., 2012; van den Wildenberg et al., 2006, Swann et al., 2011) and have been shown to mask group effects on Flanker and Simon tasks (Wylie et al., 2009a, b, 2010a, b).

To implement the distributional analyses, single-trial RT data for each participant were rank-ordered from fastest to slowest and then divided into 7 equal-sized bins (i.e. each bin contains the same number of trials). CAFs for errors and delta plots for RT were computed from these data. For CAFs, the data from all trials, both correct and incorrect, were separated by correspondence. Mean accuracy rates were calculated for each bin and plotted as a function of the mean RT for each bin. According to the DPAS model, the strength of capture by the incorrect response impulse is reflected by the proportion of fast, impulsive errors that are easily visualized and measured in plots of accuracy rates against RT (i.e., a *Conditional Accuracy Function*) for each level of Correspondence (Kornblum et al., 1990; van den Wildenberg et al., 2010; Wylie et al., 2010a,). Accuracy rates from the fastest RT bin of the CAFs for Nc trials are the most sensitive measures of an individual's proactive control over initial response impulses (see van den Wildenberg et al., 2010).

For the delta plots, the Simon effect ($RT_{NC} - RT_{C}$, correct trials only) was calculated for each bin and plotted as a function of the mean RT for each bin. Similar to the CAFs, each bin contains an equal number of trials. In the absence of any inhibitory control, we would predict positive-going delta slopes (i.e., a linear, proportional increase in the difference between two experimental conditions across the RT distribution; Luce, 1986). According to the Dual-Process Activation-Suppression (DPAS) model, the violation of this pattern leads to the inference of an inhibitory mechanism engaged to suppress the interference (Ridderinkhof, 2002). The DPAS also asserts that the proficiency of inhibitory control is most evident at the slow end of the RT distribution because it takes time for this control to build up after it has been triggered by the conflicting response impulse. Plotting the magnitude of the Simon interference effect (RT Nc trials minus RT Cs trials) as a function of response speed (i.e., a *delta plot*) yields a pattern of increasing interference across fast to intermediate response latencies that is followed by a dramatic and statistically deviant reduction (c.f., Luce, 1986) in interference toward the slow end of the distribution (Proctor et al., 2011).

The DPAS model asserts that the slope of the interference reduction at the slowest segment of the delta plot (i.e. slope between the last two bins) provides the most sensitive metric of the proficiency of inhibitory control over conflicting motor impulses, an assertion supported empirically across several studies using both non-clinical and clinical populations (Burle et

al., 2002; Ridderinkhof et al., 2005; Bub et al., 2006; Wijnen and Ridderinkhof, 2007; Wylie et al., 2009a, b, 2010a, b, 2005; for review, see van den Wildenberg et al., 2010).

The first set of analyses compared Parkinson's disease participants in their dopamine withdrawn state (i.e., "off" DBS, "off" dopamine state) and HC participants on mean interference effects (RT, accuracy), impulse capture (CAF), and proficiency of inhibitory control (delta plot) using separate repeated-measures ANOVAs and *t*-tests as appropriate. The second set of analyses focused on Parkinson's disease participants and tested the effects of *DBS State* (OFF, Chronic ON, Acute ON) on these measures.

2.1.4. Results

2.1.4.1. Analysis of sample demographics: Table 1 shows that HC and Parkinson's disease patients were similar in age, education, and gender distribution (all *p*s > .1). Table 2 shows clinical stimulation settings for Experiment 1 and 2.

Performance of Parkinson's disease Patients "Off" DBS and "Off" Dopamine Medications Versus HC

2.1.4.1.1. Mean interference effects on RT and accuracy (Fig. 1a and b): Overall, Parkinson's disease patients in their withdrawn (i.e., off DBS and off medication) state were 107 ms slower to respond than HCs, but equally as accurate ([PD vs. HC: RT 588 vs. 481 ms; Accuracy 96.49 vs. 96.82%] *Group*: RT, $F(1,32) = 22.42$, $p < .001$; Accuracy, $F(1,32) = .1$, $p = .74$). A robust Simon effect was produced across participants, which was revealed by reactions that averaged 37 ms slower and 2.5% less accurate for Nc compared to Cs trials, (*Correspondence*: RT, $F(1,32) = 153.72$, $p < .001$); Accuracy, $F(1,32) = 12.74$, $p < .01$). The magnitude of the overall Simon effect on RT and accuracy was similar across Parkinson's disease patients (38 ms) and HCs (37 ms), (PD: 2.1%; HC: 2.9%), (*GroupxCorrespondence*: RT, $F(1,32) = .01$, $p = .93$; Accuracy, $F(1,32) = .28$, $p = .60$).

2.1.4.1.2. Response capture by incorrect action impulses (Fig. 2): Consistent with the DPAS model, the CAF plot (Fig. 2a) shows that most errors occurred on the fastest reactions in the Nc condition, suggesting that the impulsive response captured the motor system sufficiently to produce overt response errors. Analysis of the fastest bin of trials confirmed a higher percentage of fast impulsive errors on Nc compared to Cs trials (*Correspondence*, $F(1,32) = 18.96$, $p < .001$) which did not differ across *Groups* (*GroupxCorrespondence*, $F(1,32) = 1.04$, $p = .32$). Within the conceptual framework of the DPAS model, this indicates that the strength of capture by incorrect response impulses was similar across Parkinson's disease and HC groups.

2.1.4.1.3. Suppressing interference from action impulses (Fig. 3): The slope of interference reduction (i.e., final delta plot slope) used to infer the proficiency of inhibitory control was significantly less steep, and in fact a positive slope, for Parkinson's disease patients ($m = .03$) compared to a steeply negative slope for HCs ($m = -.30$) $t(32) = 3.18$, $p < .01$). According to the DPAS model, this suggests that Parkinson's disease patients withdrawn from dopamine medications and from DBS were less effective at inhibiting interference from action

impulses compared to HCs, a finding that replicates several prior studies of Parkinson's disease (van Wouwe et al., 2016; Wylie et al., 2012a, b).

Performance of PD Participants in "Off", "Chronic On", and "Acute On" DBS States

2.1.4.1.4. Mean interference effects on rt and accuracy (Fig. 1): Overall, reaction times (RTs), but not response accuracies, varied by DBS state, with *chronic* and *acute* STN DBS states producing a similar, roughly 45 ms, speeding of RTs compared to the DBS off state (*DBS State*: RT, $F(2,22)=7.07$, $p < .01$; Accuracy, $F(2,22)=.49$, $p=.62$). A robust Simon effect was produced across all STN DBS states, which was revealed by reactions that were, on average, 28 ms slower and 2.5% less accurate for Nc compared to Cs trials, (*Correspondence*: RT, $F(1,11)=38.56$, $p < .001$; Accuracy, $F(1,11)=8.86$, $p < .05$). The magnitude of the Simon effect on mean RT and on mean accuracy rates did not vary as a function of STN DBS state (*DBS State x Correspondence*: RT, $F(2,22)=1.42$, $p=.26$; Accuracy, $F(2,22)=.41$, $p=.67$).

2.1.4.1.5. Response capture by incorrect action impulses (Fig. 2): A focused analysis on the fastest bin of accuracy rates confirmed that the higher percentage of fast impulsive errors on Nc compared to Cs trials (*Correspondence* $F(1,11)=15.57$, $p < .01$) was similar across DBS states (*DBS State*, $F(2,22)=2.59$, $p=.1$; *DBS State x Correspondence*, $F(2,22)=.31$, $p=.73$). Within the conceptual framework of the DPAS model, these results suggest that the strength of *impulse capture* by incorrect responses was unaffected by STN DBS states in the current investigation. Visual inspection suggests that RTs in the first bin are different across DBS State, therefore we applied a post-hoc analysis to check this. Patients Off DBS were significantly slower (398 ms) in comparison to participants with chronic (345 ms, $F(1,11)=15.6$, $p < .01$) and acute DBS (350 ms, $F(1,11)=12.0$, $p < .01$), independent of Correspondence, *DBS State x Correspondence*, $F(2,22)=.28$, $p=.76$).

2.1.4.1.6. Suppressing interference from action impulses (Fig. 3): The proficiency of reactive inhibitory control (i.e., slope of interference reduction in final delta plot segment) was significantly improved (i.e., more steeply negative) in the *Chronic* ($m=-.24$, $F(1,11)_{\text{Chronic-Off}}=8.88$, $p < .05$) and in the *Acute* STN DBS state ($m=-.22$, *DBS State*, $F(1,11)_{\text{Acute-Off}}=5.5$, $p < .05$) compared to the OFF state ($m=.03$). According to the DPAS model, these patterns confirm that Parkinson's disease patients were more effective at suppressing interference from action impulses when STN DBS was ON compared to OFF, a finding that replicates prior findings in dopamine medicated Parkinson's disease patients.

3. Experiment 2

3.1. Methods

3.1.1. Participants—We recruited a new sample of Parkinson's disease participants (n=11) who had bilateral STN DBS implants. We used identical recruitment and inclusion/exclusion criteria, informed consent procedures, and dopamine medication withdrawal procedures as outlined in Experiment 1.

3.1.2. DBS contact registration and selection procedures—Each patient had pre-operative MRI (T1 and T2) acquisitions of the brain as well as a delayed post-operative CT acquired approximately one month after surgery. Typical CT images were acquired at kVp =120 V, exposure 350 mAs and 512×512 pixels. In-plane resolution and slice thickness were approximately .5 mm and .75 mm, respectively. MRI T1 (TR 7.9 ms, TE 3.8 ms, 256×256×170 voxels, with typical voxel resolution of 1×1×1 mm3) were acquired using the SENSE parallel imaging technique (T1W/3D/TFE) from Philips on a 3 T scanner. MRI T2 (TR 3000 ms, TE 80 ms, 512×512×45 voxels, with typical voxel resolution of .47×.47×2 mm3) were acquired using the SENSE parallel imaging technique (T2W/TSE) from Philips on a 3 T scanner. Using the CranialVault Explorer software (D'Haese et al., 2012), the implants and individual contacts were automatically localized and manually checked. The PREOP MRIs as well as the POSTOP CT were also aligned to each other using fully-automatic intensity-based rigid registration techniques available in CRAVE. This enabled visualization of the implants and individual contacts on the anatomical MRI images of the patient. The average inter-rate difference (between two experts) in localization of contacts on the implants from the POSTOP CT after automatic localization was .4 mm (SD =.08 mm) agreement. The PREOP MRI was aligned to the CranialVault atlas using fully-automatic intensity-based non-linear image registration technique available in CRAVE (Rohde et al., 2003). This enabled automatic atlas-based segmentation of the STN in the patient (D'Haese et al., 2005, Pallavaram et al., 2015, 2009). The segmented STN visualized on the patient T1 and T2 MRI scans was further divided along the dorsolateral and ventromedial axis (along the lines of the subdivision defined by Haynes and Haber, 2013). By analyzing the implant in every case with respect to the segmented STN, patients were recruited for the study whose bilateral leads contained at least one contact centered in the dorsal and one contact centered in the ventral subregion of the STN, see Fig. 4 for the electrode contacts embedded in dorsal and ventral regions of the STN and Fig. 5 for visualization of the STN subregions at different planes. For a comparison between experiments with respect to electrode locations, see Fig. 6, which shows the cluster of clinically active electrode contacts embedded in the STN from the subjects with available MRI and CT data (8) from Experiment 1.

Experimental Design and Procedure Participants performed the Simon task twice, once while DBS was applied to dorsal STN contacts bilaterally and once while DBS was applied to ventral STN contacts bilaterally. The patients were kept blind to the simulation conditions in each session. After the cognitive testing, the UPDRS was administered. The order of stimulation in dorsal versus ventral STN was counterbalanced across patients, and a 30-min waiting period was inserted after each programming change, before the first session and in between sessions. Typical clinical settings use parameters that inevitably produce large stimulation fields. Here we equated stimulation across patients using a constant current of .4 mA while holding stimulation frequency at 130 Hz and pulsewidth of 60 μs. This setting was chosen to provide (to the extent possible) uniform current density across subregions and patients. The aim was to restrict the estimated field of neural tissue activation in order to provide greater selectivity in stimulating subregions. Based on Butson & McIntyre (2008) a stimulation amplitude of approximately .4 mA (with an average clinical impedance of 1 kΩ) would result in a radius of the volume of activated tissue (VTA) of about 1.3 mm. Note that the center to center distance from electrode contacts is 2 mm (i.e. 1.5 mm contacts spaced .5

mm apart). A VTA with 1.3 mm radius would thus lead to minimal overlap in activated tissue between neighboring electrode points, see Fig. 7a and b for an example of the estimated VTA with average clinical stimulation settings for experiment 1 in comparison to the experimentally controlled VTA of experiment 2. Table 3 provides the contact points that were stimulated as part of the dorsal and ventral stimulation condition, separate for left and right electrodes. Summarized, the combination of selecting contacts a priori that were situated in relatively dorsal and ventral STN subregions and focusing the stimulation in those regions provided higher fidelity stimulation in distinct STN subregions.

3.1.3. Statistical analyses—We compared the within-subject effect of stimulating dorsal and ventral STN subregions on mean interference effects (RT, accuracy), impulse capture (CAF), and proficiency of inhibitory control (delta plot) using repeated-measures ANOVAs and *t*-tests as appropriate.

3.1.4. Results

3.1.4.1. Analysis of sample demographics: Table 1 shows age, education, gender distribution, and key clinical characteristics for experiment 2. Table 2 shows clinical stimulation settings for both experiments.

Within-Subject Comparison of Stimulation Effects in Dorsal Versus Ventral STN.

3.1.4.1.1. Mean interference effects on RT and accuracy (Fig. 8): RTs, but not response accuracy, varied by DBS stimulation region, with ventral STN stimulation producing significantly faster RTs than dorsal STN stimulation (*DBS Subregion:* RT, $F(1,10)=6.31$, $p < .05$; Accuracy, $F(1,10)=3.38$, $p=.1$). A robust Simon effect was produced across both stimulation sites, which was revealed by reactions that averaged 50 ms slower and 4.2% less accurate for Nc compared to Cs trials (*Correspondence*: RT, $F(1,10)=134.8$, $p < .001$; Accuracy, $F(1,11)=6.41$, $p < .05$). The magnitude of the Simon effect on mean RT and on mean accuracy rates did not vary as a function of the *Subregion* that was stimulated (*Subregion x Correspondence*: RT, $F(1,10)=1.25$, $p=.92$; Accuracy, $F(1,10)=.32$, $p=.58$).

3.1.4.1.2. Response capture by incorrect action impulses (Fig. 9): The analysis of the fastest bin of accuracy rates revealed the expected higher percentage of fast impulsive errors on Nc than on Cs trials (*Correspondence,* $F(1,10)=9.7$, $p < .05$), a pattern that did not vary by the stimulated subregion (*Subregion* ($F(1,10)=.24$, $p=.64$; *Subregion x Correspondence*, $F(1, 10)=.30$, $p=.60$). This indicates that the strength of *impulse capture* by incorrect responses was not directly modulated by focused stimulation in dorsal versus ventral STN subregions.

3.1.4.1.3. Suppressing interference from action impulses (Fig. 10): The proficiency of inhibitory control revealed by slope reduction of interference at the tail end of the delta plot was significantly more negative-going when DBS was applied to the dorsal STN subregion (m =−.24) compared to stimulation of the ventral STN subregion ($m=.04$, $t(10)=2.61$, $p < .05$). These patterns show that Parkinson's disease patients were more effective at inhibiting interference from action impulses with targeted stimulation in the dorsal as opposed to the ventral STN.

4. Discussion

We replicated and extended previous findings by demonstrating that DBS applied using clinical settings improves reactive inhibitory control of response impulses in Parkinson's disease patients withdrawn from the influence of dopamine medications. Moreover, we showed that selectively stimulating the dorsal as opposed to the ventral STN substructure is responsible for this effect. This provides new evidence that dorsal STN circuitries play a key role in the suppression of motor impulses.

4.1. Effects of DBS STN on proactive impulse control (impulse capture)

We reported previously that Parkinson's disease patients ON STN stimulation demonstrated poorer *proactive impulse control* (i.e., increased *impulse capture*) compared to OFF stimulation, and several other studies of STN DBS across a variety of reaction time paradigms have shown increased impulsive errors (Wylie et al., 2010a, b; Campbell et al., 2008; Ballanger et al., 2009; Hershey et al., 2004; Jahanshahi et al., 2000; Witt et al., 2004). Although clinical DBS did not increase impulsive errors relative to HC, DBS significantly sped up RTs and made patients relatively (but not significantly) more error prone than without DBS. Thus, the direction of these results is in line with previous findings in Parkinson's disease and with human imaging studies suggestive that DBS modulates circuitry linking pre-supplementary motor area and STN, which lowers response thresholds and induces a shift in speed-accuracy tradeoffs (Forstmann 2008a, b, c; Frank et al., 2007; Ballanger et al., 2009, Wylie et al., 2010a, b). A prior study found increases in response commission errors in a go/no-go paradigm when directing stimulation to a relatively more ventral contact, but DBS was applied at clinical settings and to contacts often outside of the STN structure (Hershey et al., 2004). While we addressed some of these issues, we did not observe differences in fast impulsive error rates when focusing DBS in dorsal versus ventral STN subregions.

One potentially relevant confound across studies is uncertainty regarding the interactive effects of dopaminergic medication and STN stimulation, other stimulation parameters that might affect proactive impulse control but we did not control for in the current experiment, like the laterality of electrode positioning, and the frequency settings of stimulation which require further investigation. Variability in STN DBS-induced impulsive errors also depends on the prepotency of the go reaction and the time pressure to make decisions, further pointing to a role for STN DBS in adjusting response and decision thresholds (Georgiev et al., 2016; Jahanshahi et al., 2015). Future studies manipulating speed-accuracy instructions or the probabilities of corresponding and non-corresponding Simon task trials combined with dorsal and ventral stimulation could provide further insight about the role of DBS to STN subregions in modulating proactive control of strong response impulses.

4.2. Effects of DBS STN on reactive inhibitory control

STN DBS applied using clinical settings significantly improved the proficiency of reactive inhibitory control in a group of Parkinson's disease patients withdrawn from dopaminergic medications. This replicates previous studies of DBS in medicated Parkinson's disease patients on several reactive inhibitory control measures, that is, clinical DBS both improved

selective suppression of irrelevant motor impulses in the Simon task (Wylie et al., 2010a, b) as well as global action cancelation as measured by the Stop task (Mirabella et al., 2012; Swann et al., 2011; van den Wildenberg et al., 2006).

While a limitation is that long-term dopaminergic therapy on inhibitory control circuitry cannot be addressed in this study, the replicated effect in the absence of dopamine replacement therapy strengthens the hypothesis that STN DBS directly modulates inhibitory control circuitries. In sum, our findings provide strong support that improved selective suppression with clinical STN stimulation is not a by-product of interrupted stimulation effects or of dopamine medication state.

Most importantly, we show that focusing stimulation to a dorsal STN subregion has the direct and dramatic effect of improving the proficiency of inhibiting interference from impulsive responses. Stimulating a ventral STN subregion showed minimal suppression of interference.

A limitation is that we did not measure cognitive or motor performance in an OFF DBS state in Experiment 2. However, note that ventral STN stimulation showed a suppression pattern similar to DBS OFF states from Experiment 1 and our prior study (Wylie et al., 2010a, b). Unlike what would be expected according to performance pattern in the OFF state in experiment 1, ventral stimulation induced faster instead of slower RTs compared to dorsal stimulation. Faster RTs have been previously associated with reduced suppression, however, the overall pattern of performance with ventral versus dorsal STN stimulation does not seem to be explained by a global shift in the speed-accuracy trade off since fast impulsive errors and RTs in the fastest portion of the distributions were similar across stimulation conditions (Wylie et al., 2009a, b; van Wouwe et al., 2014).

With respect to the absence of UPDRS scores in the OFF state in Experiment 2; UPDRS scores in dorsal and ventral stimulation both seem fairly close to the OFF state of Experiment 1, which suggest that STN subregion stimulation did not improve motor symptoms. Although this limits the clinical application of the settings used in Experiment 2, it does not exclude linking STN subregions to inhibitory action control. Dissociations between motor networks and other functions (emotion) have been found by Campbell et al. (2012) who showed that there were no consistent relations between DBS related improvements in UPDRS and mood. Similarly, in Experiment 1, we found no correlations between improvement in UPDRS improvement and action control from OFF to ON state (OFF-Chronic, $r=-.39$, $p=.3$; OFF-Acute, $r=-.36$, $p=.35$).

The findings from Experiment 2 implicate circuitry intersecting the dorsal STN subterritories as playing a critical role in selective response inhibition of strong motor impulses. The relatively dorsal STN substructure is innervated by projections from prefrontal cortical areas (e.g., pre-supplementary motor area, inferior frontal cortex) that have been associated previously with inhibitory control broadly (action cancelation and suppression of conflicting responses) as well as reactive inhibition of response impulses in the Simon task (Forstmann, 2008a, b, c). Recent studies suggest that modulatory effects of DBS on cognitive control circuitries might involve complex changes in STN firing rates and

oscillatory activities. Increased firing rates in STN have been timed to inhibitory motor control in inhibition paradigms (Schmidt et al., 2013). Zavala et al. (2015) proposed recently that oscillatory activity in theta and beta frequency bands reflecting communication between frontal cortex (Medial Prefrontal Cortex and Inferior Frontal Cortex) and STN play important roles, respectively, in delaying responses in times of conflict and stopping or terminating actions. Similarly, Accolla et al. (2016) proposed that beta oscillatory activity may be differentially expressed and functionally distinct across STN subregions. In particular, source localization showed that beta oscillatory was significantly higher at dorsal in comparison to ventral STN DBS lead contacts. The dorsal STN also showed connectivity with motor, premotor, prefrontal areas, whereas the more ventral area was linked to hippocampus and amygdala. Thus, there may also be distinct STN subregions and neurophysiological patterns that correspond to the improved reactive inhibitory control as reported in the current study. Establishing links between inhibitory control of selective action impulses versus global action cancelation as measured by Zavala et al. (2015) and Accolla et al., (2016) and neurophysiological patterns in distinct STN subregions awaits future investigation.

In conclusion, we provide direct evidence that stimulating the STN, and specifically the dorsal substructure, improves the proficiency of inhibiting response impulses. As advances in DBS technology allow for more precise stimulation and even closed-loop stimulation capabilities, mapping out linkages between motor and cognitive processes and stimulation parameters (e.g., subregions, oscillatory bands, etc.) is critical for expanding our treatment of PD and related basal ganglia disorders.

Acknowledgments

Funding

Some of the work done using the CranialVault atlas, showing the normalized centroids overlaid on anatomical segmentations, was supported by NIH R01-EB006136 and R01-NS095291 (to B.D.). M.S.O. DBS research was supported by R01 NR014852 and R01NS096008.

We thank Bert van Beek for programming the computer task. The authors would also like to acknowledge the support of the National Parkinson Foundation, Tyler’s Hope and the Bachmann-Strauss Foundation, UF Foundation, and the UF INFORM database to the University of Florida Center for Movement Disorders and Neurorestoration.

Abbreviations

CAF	Conditional Accuracy Function
CRAVE	CranialVault Explorer
Cs	Corresponding
DA	Dopamine
DPAS	Dual-Process Activation-Suppression
DBS	Deep Brain Stimulation
HC	Healthy Controls

Nc	Non-Corresponding
PD	Parkinson's disease
RT	Reaction Time
STN	Subthalamic Nucleus

References

Accolla EA, Herrojo Ruiz M, Horn A, Schneider GH, Schmitz-Hübsch T, Draganski B, Kühn AA. Brain Networks Modulated by Subthalamic Nucleus Deep Brain Stimulation. Brain. 2016

Aron AR, Durston S, Eagle DM, Logan GD, Stinear CM, Stuphorn V. Converging evidence for a fronto-basal-ganglia network for inhibitory control of action and cognition. J Neurosci. 2007; 27:11860–11864. [PubMed: 17978025]

Aron AR, Poldrack RA. Cortical and subcortical contributions to Stop signal response inhibition: role of the subthalamic nucleus. J Neurosci. 2006; 26:2424–2433. [PubMed: 16510720]

Ballanger B, van Eimeren T, Moro E, Lozano AM, Hamani C, Boulinguez P, Pellecchia G, Houle S, Poon YY, Lang AE, Strafella AP. Stimulation of the subthalamic nucleus and impulsivity: release your horses. Ann Neurol. 2009; 66:817–824. [PubMed: 20035509]

Beck AT, Ward CH, Mendelson M, Mock J, Erbaugh J. An inventory for measuring depression. Arch Gen Psychiatry. 1961; 44:53–62.

Botvinick MM, Braver TS, Barch DM, Carter CS, Cohen JD. Conflict monitoring and cognitive control. Psychol Rev. 2001; 108:624–652. [PubMed: 11488380]

Bub DN, Masson ME, Lalonde CE. Cognitive control in children: stroop interference and suppression of word reading. Psychol Sci. 2006; 17:351–357. [PubMed: 16623694]

Burle B, Possamaï CA, Vidal F, Bonnet M, Hasbroucq T. Executive control in the Simon effect: an electromyographic and distributional analysis. Psychol Res. 2002; 66:324–336. [PubMed: 12466929]

Butson CR, McIntyre CC. Current steering to control the volume of tissue activated during deep brain stimulation. Brain Stimul. 2008; 1(1):7–15. http://dx.doi.org/10.1016/j.brs.2007.08.004. [PubMed: 19142235]

Campbell MC, Karimi M, Weaver PM, Wu J, Perantie DC, Golchin NA, Tabbal SD, Perlmutter JS, Hershey T. Neural correlates of STN DBS-induced cognitive variability in Parkinson disease. Neuropsychologia. 2008; 46:3162–3169. [PubMed: 18682259]

Campbell MC, Black KJ, Weaver PM, Lugar HM, Videen TO, Tabbal SD, et al. Mood response to deep brain stimulation of the subthalamic nucleus in Parkinson's disease. J Neuropsychiatry Clin Neurosci. 2012; 24(1):28–36. [PubMed: 22450611]

Cavanagh JF, Zambrano-Vazquez L, Allen JJ. Theta lingua franca: a common mid-frontal substrate for action monitoring processes. Psychophysiology. 2012; 49:220–238. [PubMed: 22091878]

D'Haese PF, Cetinkaya E, Konrad PE, Kao C, Dawant BM. Computer-aided placement of deep brain stimulators: from planning to intraoperative guidance. IEEE Trans Med Imaging. 2005; 24:1469–1478. [PubMed: 16279083]

D'Haese PF, Pallavaram S, Li R, Remple MS, Kao C, Neimat JS, Konrad PE, Dawant BM. CranialVault and its CRAVE tools: a clinical computer assistance system for deep brain stimulation (DBS) therapy. Med Image Anal. 2012; 16:744–753. [PubMed: 20732828]

Eagle DM, Baunez C. Is there an inhibitory-response-control system in the rat? evidence from anatomical and pharmacological studies of behavioral inhibition. Neurosci Biobehav Rev. 2010; 34:50–72. [PubMed: 19615404]

Folstein MF, Folstein SE, McHugh PR. "Mini-mental state" A practical method for grading the cognitive state of patients for the clinician. J Psychiatr Res. 1975; 12:189–198. [PubMed: 1202204]

Forstmann BU, Dutilh G, Brown S, Neumann J, von Cramon DY, Ridderinkhof KR, Wagenmakers EJ. Striatum and pre-SMA facilitate decision-making under time pressure. Proc Natl Acad Sci USA. 2008a; 105:17538–17542. [PubMed: 18981414]

Forstmann BU, Jahfari S, Scholte HS, Wolfensteller U, van den Wildenberg WP, Ridderinkhof KR. Function and structure of the right inferior frontal cortex predict individual differences in response inhibition: a model-based approach. J Neurosci. 2008b; 28:9790–9796. [PubMed: 18815263]

Forstmann BU, van den Wildenberg WP, Ridderinkhof KR. Neural mechanisms, temporal dynamics, and individual differences in interference control. J Cogn Neurosci. 2008c; 20:1854–1865. [PubMed: 18370596]

Frank MJ, Claus ED. Anatomy of a decision: striato-orbitofrontal interactions in reinforcement learning, decision making, and reversal. Psychol Rev. 2006; 113:300–326. [PubMed: 16637763]

Frank MJ, Samanta J, Moustafa AA, Sherman SJ. Hold your horses: impulsivity, deep brain stimulation, and medication in parkinsonism. Science. 2007; 318(5854):1309–1312. http://dx.doi.org/10.1126/science.1146157. [PubMed: 17962524]

Georgiev D, Dirnberger G, Wilkinson L, Limousin P, Jahanshahi M. In Parkinson's disease on a probabilistic Go/NoGo task deep brain stimulation of the subthalamic nucleus only interferes with withholding of the most prepotent responses. Exp Brain Res. 2016; 234:1133–1143. [PubMed: 26758720]

Gillan CM, Papmeyer M, Morein-Zamir S, Sahakian BJ, Fineberg NA, Robbins TW, de Wit S. Disruption in the balance between goal-directed behavior and habit learning in obsessive-compulsive disorder. Am J Psychiatry. 2011; 168:718–726. [PubMed: 21572165]

Greenhouse I, Gould S, Houser M, Aron AR. Stimulation of contacts in ventral but not dorsal subthalamic nucleus normalizes response switching in Parkinson's disease. Neuropsychologia. 2013; 51:1302–1309. [PubMed: 23562963]

Greenhouse I, Gould S, Houser M, Hicks G, Gross J, Aron AR. Stimulation at dorsal and ventral electrode contacts targeted at the subthalamic nucleus has different effects on motor and emotion functions in Parkinson's disease. Neuropsychologia. 2011; 49:528–534. [PubMed: 21184765]

Haynes WI, Haber SN. The organization of prefrontal-subthalamic inputs in primates provides an anatomical substrate for both functional specificity and integration: implications for basal ganglia models and deep brain stimulation. J Neurosci. 2013; 33:4804–4814. [PubMed: 23486951]

Hershey T, Campbell MC, Videen TO, Lugar HM, Weaver PM, Hartlein J, Karimi M, Tabbal SD, Perlmutter JS. Mapping Go-No-Go performance within the subthalamic nucleus region. Brain. 2010; 133:3625–3634. [PubMed: 20855421]

Hershey T, Revilla FJ, Wernle A, Gibson PS, Dowling JL, Perlmutter JS. Stimulation of STN impairs aspects of cognitive control in PD. Neurology. 2004; 62:1110–1114. [PubMed: 15079009]

Holl AK, Wilkinson L, Tabrizi SJ, Painold A, Jahanshahi M. Selective executive dysfunction but intact risky decision-making in early Huntington's disease. Mov Disord. 2013; 28:1104–1109. [PubMed: 23436289]

Jahanshahi M, Ardouin CM, Brown RG, Rothwell JC, Obeso J, Albanese A, Rodriguez-Oroz MC, Moro E, Benabid AL, Pollak P, Limousin-Dowsey P. The impact of deep brain stimulation on executive function in Parkinson's disease. Brain. 2000; 123(Pt 6):1142–1154. [PubMed: 10825353]

Jahanshahi M, Obeso I, Baunez C, Alegre M, Krack P. Parkinson's disease, the subthalamic nucleus, inhibition, and impulsivity. Mov Disord. 2015; 30:128–140. [PubMed: 25297382]

Jahfari S, Waldorp L, van den Wildenberg WP, Scholte HS, Ridderinkhof KR, Forstmann BU. Effective connectivity reveals important roles for both the hyperdirect (fronto-subthalamic) and the indirect (fronto-striatal-pallidal) fronto-basal ganglia pathways during response inhibition. J Neurosci. 2011; 31:6891–6899. [PubMed: 21543619]

Keuken MC, Uylings HB, Geyer S, Schafer A, Turner R, Forstmann BU. Are there three subdivisions in the primate subthalamic nucleus? Front Neuroanat. 2012; 6:14. [PubMed: 22590455]

Kolomiets BP, Deniau JM, Mailly P, Ménétrey A, Glowinski J, Thierry AM. Segregation and convergence of information flow through the cortico-subthalamic pathways. J Neurosci. 2001; 21:5764–5772. [PubMed: 11466448]

Konrad PE, Neimat JS, Yu H, Kao CC, Remple MS, D'Haese PF, Dawant BM. Customized, miniature rapid-prototype stereotactic frames for use in deep brain stimulator surgery: initial clinical methodology and experience from 263 patients from 2002 to 2008. Stereo Funct Neurosurg. 2011; 89:34–41.

Kornblum S, Hasbroucq T, Osman A. Dimensional overlap: cognitive basis for stimulus-response compatibility–a model and taxonomy. Psychol Rev. 1990; 97:253–270. [PubMed: 2186425]

Lopiano L, Torre E, Benedetti F, Bergamasco B, Perozzo P, Pollo A, Rizzone M, Tavella A, Lanotte M. Temporal changes in movement time during the switch of the stimulators in Parkinson's disease patients treated by subthalamic nucleus stimulation. Eur Neurol. 2003; 50:94–99. [PubMed: 12944714]

Luce, RD. Response times: their role in inferring elementary mental organization. Oxford Science Publications; New York: 1986.

Mansfield EL, Karayanidis F, Jamadar S, Heathcote A, Forstmann BU. Adjustments of response threshold during task switching: a model-based functional magnetic resonance imaging study. J Neurosci. 2011; 31:14688–14692. [PubMed: 21994385]

Mirabella G, Iaconelli S, Romanelli P, Modugno N, Lena F, Manfredi M, Cantore G. Deep brain stimulation of subthalamic nuclei affects arm response inhibition in Parkinson's patients. Cereb Cortex. 2012; 22:1124–1132. [PubMed: 21810782]

Nambu A, Tokuno H, Takada M. Functional significance of the cortico-subthalamo-pallidal 'hyperdirect' pathway. Neurosci Res. 2002; 43:111–117. [PubMed: 12067746]

Pallavaram S, Dawant BM, Koyama T, Yu H, Neimat J, Konrad PE, D'Haese PF. Validation of a fully automatic method for the routine selection of the anterior and posterior commissures in magnetic resonance images. Stereo Funct Neurosurg. 2009; 87:148–154.

Pallavaram S, D'Haese PF, Lake W, Konrad PE, Dawant BM, Neimat JS. Fully automated targeting using nonrigid image registration matches accuracy and exceeds precision of best manual approaches to subthalamic deep brain stimulation targeting in Parkinson disease. Neurosurgery. 2015; 76:756–765. [PubMed: 25988929]

Proctor RW, Miles JD, Baroni G. Reaction time distribution analysis of spatial correspondence effects. Psychon Bull Rev. 2011; 18:242–266. [PubMed: 21327376]

Radloff LS. The CES-D scale: a self-report depression scale for research in the general population. Appl Psychol Meas. 1977; 1:385–401.

Ridderinkhof KR. Micro- and macro-adjustments of task set: activation and suppression in conflict tasks. Psychol Res. 2002; 66:312–323. [PubMed: 12466928]

Ridderinkhof KR, Scheres A, Oosterlaan J, Sergeant JA. Delta plots in the study of individual differences: new tools reveal response inhibition deficits in AD/Hd that are eliminated by methylphenidate treatment. J Abnorm Psychol. 2005; 114:197–215. [PubMed: 15869351]

Ridderinkhof KR, van den Wildenberg WP, Segalowitz SJ, Carter CS. Neurocognitive mechanisms of cognitive control: the role of prefrontal cortex in action selection, response inhibition, performance monitoring, and reward-based learning. Brain Cogn. 2004; 56:129–140. [PubMed: 15518930]

Schmidt R, Leventhal DK, Mallet N, Chen F, Berke JD. Canceling actions involves a race between basal ganglia pathways. Nat Neurosci. 2013; 16:1118–1124. [PubMed: 23852117]

Swann N, Poizner H, Houser M, Gould S, Greenhouse I, Cai W, Strunk J, George J, Aron AR. Deep brain stimulation of the subthalamic nucleus alters the cortical profile of response inhibition in the beta frequency band: a scalp EEG study in Parkinson's disease. J Neurosci. 2011; 31:5721–5729. [PubMed: 21490213]

Temperli P, Ghika J, Villemure JG, Burkhard PR, Bogousslavsky J, Vingerhoets FJ. How do parkinsonian signs return after discontinuation of subthalamic DBS? Neurology. 2003; 60:78–81. [PubMed: 12525722]

van den Wildenberg WP, van Boxtel GJ, van der Molen MW, Bosch DA, Speelman JD, Brunia CH. Stimulation of the subthalamic region facilitates the selection and inhibition of motor responses in Parkinson's disease. J Cogn Neurosci. 2006; 18:626–636. [PubMed: 16768365]

van den Wildenberg WP, Wylie SA, Forstmann BU, Burle B, Hasbroucq T, Ridderinkhof KR. To head or to heed? Beyond the surface of selective action inhibition: a review. Front Hum Neurosci. 2010; 4:222. [PubMed: 21179583]

van Wouwe NC, Kanoff KE, Claassen DO, Spears CA, Neimat J, van den Wildenberg WP, Wylie SA. Dissociable Effects of Dopamine on the Initial Capture and the Reactive Inhibition of Impulsive Actions in Parkinson's Disease. J Cogn Neurosci. 2016; 28(5):710–723. http://dx.doi.org/10.1162/jocn_a_00930. [PubMed: 26836515]

van Wouwe NC, van den Wildenberg WP, Claassen DO, Kanoff K, Bashore TR, Wylie SA. Speed pressure in conflict situations impedes inhibitory action control in Parkinson's disease. Biol Psychol. 2014a; 101:44–60. [PubMed: 25017503]

Waldau B, Clayton DA, Gasperson LB, Turner DA. Analysis of the time course of the effect of subthalamic nucleus stimulation upon hand function in Parkinson's patients. Stereo Funct Neurosurg. 2011; 89:48–55.

Weintraub D, Siderowf AD, Potenza MN, Goveas J, Morales KH, Duda JE, Moberg PJ, Stern MB. Association of dopamine agonist use with impulse control disorders in Parkinson disease. Arch Neurol. 2006; 63:969–973. [PubMed: 16831966]

Wijnen JG, Ridderinkhof KR. Response inhibition in motor and oculomotor conflict tasks: different mechanisms, different dynamics? Brain Cogn. 2007; 63:260–270. [PubMed: 17069944]

Witt K, Pulkowski U, Herzog J, Lorenz D, Hamel W, Deuschl G, Krack P. Deep brain stimulation of the subthalamic nucleus improves cognitive flexibility but impairs response inhibition in Parkinson disease. Arch Neurol. 2004; 61:697–700. [PubMed: 15148146]

Worbe Y, Palminteri S, Hartmann A, Vidailhet M, Lehéricy S, Pessiglione M. Reinforcement learning and Gilles de la Tourette syndrome: dissociation of clinical phenotypes and pharmacological treatments. Arch Gen Psychiatry. 2011; 68:1257–1266. [PubMed: 22147843]

Wylie SA, Claassen DO, Huizenga HM, Schewel KD, Ridderinkhof KR, Bashore TR, van den Wildenberg WP. Dopamine agonists and the suppression of impulsive motor actions in Parkinson disease. J Cogn Neurosci. 2012a; 24:1709–1724. [PubMed: 22571461]

Wylie SA, Claassen DO, Kanoff KE, Ridderinkhof KR, van den Wildenberg WP. Impaired inhibition of prepotent motor actions in patients with Tourette syndrome. J Psychiatry Neurosci. 2013; 38:349–356. [PubMed: 23820185]

Wylie SA, Ridderinkhof KR, Bashore TR, van den Wildenberg WP. The effect of Parkinson's disease on the dynamics of on-line and proactive cognitive control during action selection. J Cogn Neurosci. 2010a; 22:2058–2073. [PubMed: 19702465]

Wylie SA, Ridderinkhof KR, Elias WJ, Frysinger RC, Bashore TR, Downs KE, van Wouwe NC, van den Wildenberg WP. Subthalamic nucleus stimulation influences expression and suppression of impulsive behaviour in Parkinson's disease. Brain. 2010b; 133:3611–3624. [PubMed: 20861152]

Wylie SA, Stout JC, Bashore TR. Activation of conflicting responses in Parkinson's disease: evidence for degrading and facilitating effects on response time. Neuropsychologia. 2005; 43:1033–1043. [PubMed: 15769489]

Wylie SA, van den Wildenberg W, Ridderinkhof KR, Claassen DO, Wooten GF, Manning CA. Differential susceptibility to motor impulsivity among functional subtypes of Parkinson's disease. J Neurol Neurosurg Psychiatry. 2012b; 83:1149–1154. [PubMed: 22917670]

Wylie SA, van den Wildenberg WP, Ridderinkhof KR, Bashore TR, Powell VD, Manning CA, Wooten GF. The effect of Parkinson's disease on interference control during action selection. Neuropsychologia. 2009a; 47:145–157. [PubMed: 18761363]

Wylie SA, van den Wildenberg WP, Ridderinkhof KR, Bashore TR, Powell VD, Manning CA, Wooten GF. The effect of speed-accuracy strategy on response interference control in Parkinson's disease. Neuropsychologia. 2009b; 47:1844–1853. [PubMed: 19428416]

Zaghloul KA, Weidemann CT, Lega BC, Jaggi JL, Baltuch GH, Kahana MJ. Neuronal activity in the human subthalamic nucleus encodes decision conflict during action selection. J Neurosci. 2012; 32:2453–2460. [PubMed: 22396419]

Zavala B, Zaghloul K, Brown P. The subthalamic nucleus, oscillations, and conflict. Mov Disord. 2015; 30:328–338. [PubMed: 25688872]

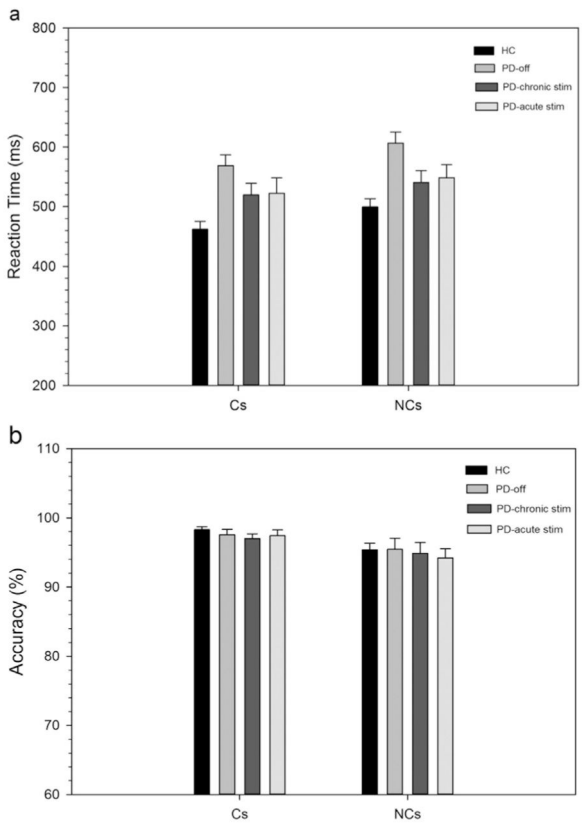

Fig. 1.

Mean RTs (1 A) and accuracy rates (1B) on corresponding (Cs) and non-corresponding (Nc) trial types for healthy controls and Parkinson's disease participants in off state and on chronic and acute STN stimulation. Error bars reflect standard error of the means.

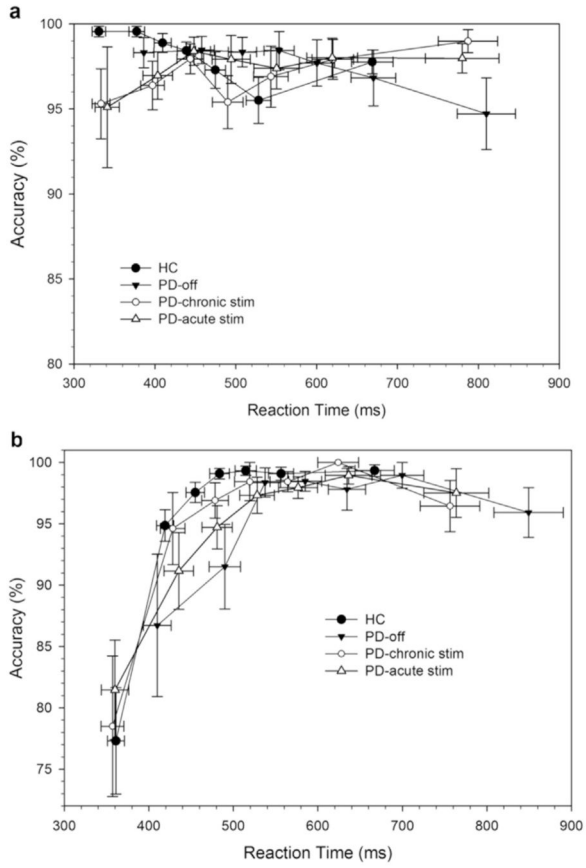

Fig. 2.

Conditional accuracy functions for corresponding (Cs, 2 A) and non-corresponding (Nc, 2B) trial types for healthy controls and Parkinson's disease participants in off state and on chronic and acute STN stimulation. Errors are predominantly associated with the fastest reaction times on non-corresponding (Nc) trials, a pattern that does not vary between groups (PD and HC) or across stimulation states. Note that each bin represents the same number of trials, averaged across the subjects in each subgroup.

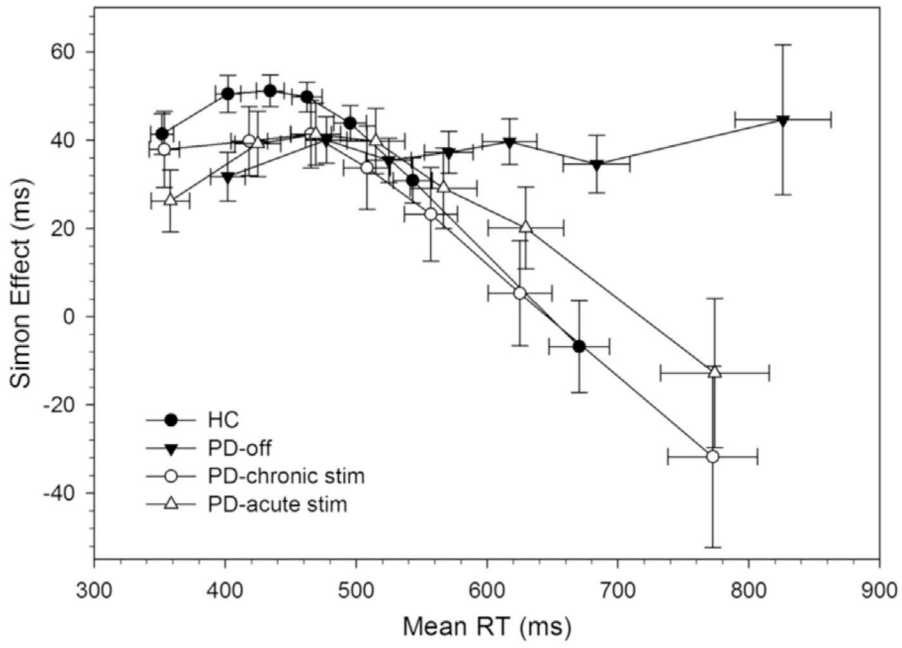

Fig. 3.

RT delta plots for healthy controls and Parkinson's disease participants in off state and on chronic and acute STN stimulation. Each bin contains the same number of trials, averaged across the subjects in each subgroup. HC show initial increase in interference followed by a drastic suppression of interference (i.e., large negative delta slope) at the slow end of the distribution. PD participants in off state show markedly less proficient suppression of interference from action impulses.

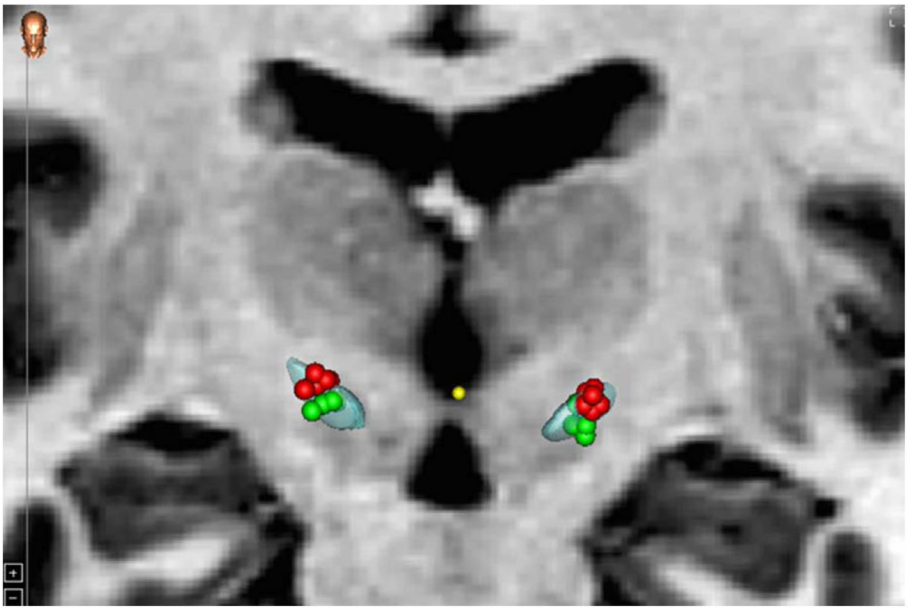

Fig. 4.

Distribution of the electrode contacts used, and projected volume of tissue activation with .4 mA, 130 Hz and 60 μs, for dorsal (red) and ventral (green) stimulation of the STN. (For interpretation of the references to color in this figure legend, the reader is referred to the web version of this article.)

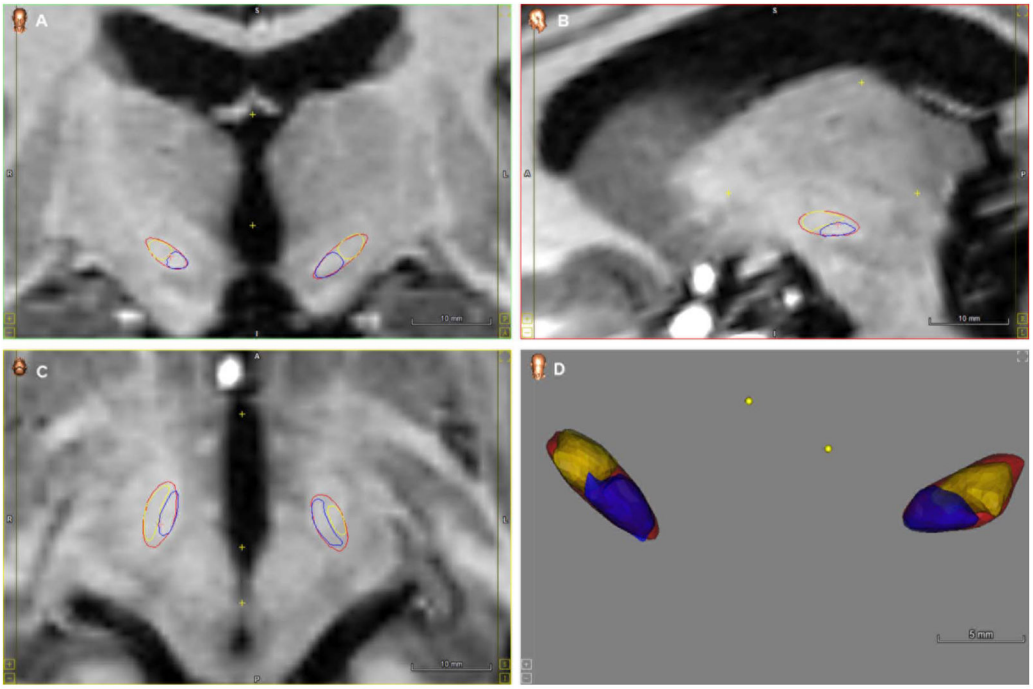

Fig. 5.

Subdivision of the STN in dorsal (yellow) and ventral (purple) to determine contact localization at different planes. Visualizations were projected on Coronal (A), Sagittal (B) and Axial plane (C) and a 3D volume (D). (For interpretation of the references to color in this figure legend, the reader is referred to the web version of this article.)

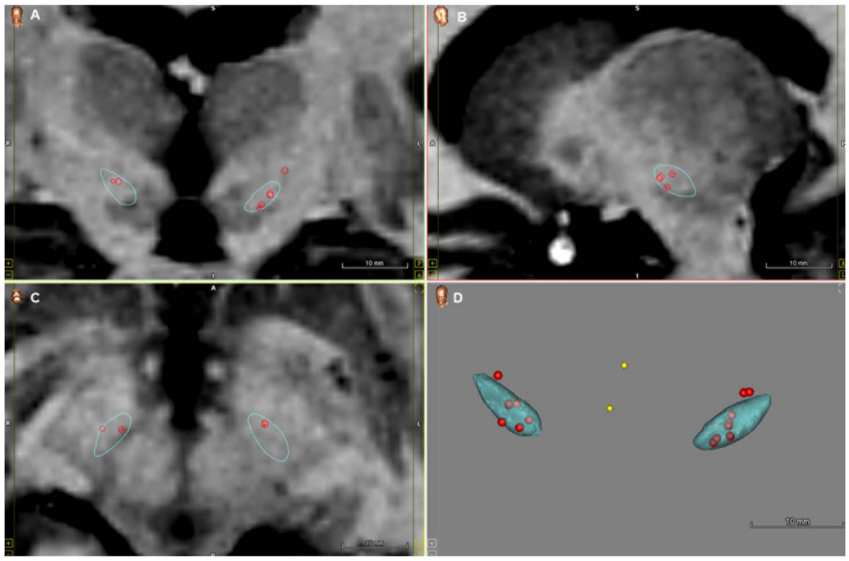

Fig. 6.

Cluster of clinically active electrode contacts embedded in the STN from a subset of subjects (n=8) from Experiment 1. Visualizations were projected on Coronal (A), Sagittal (B) and Axial plane (C) and a 3D volume (D).

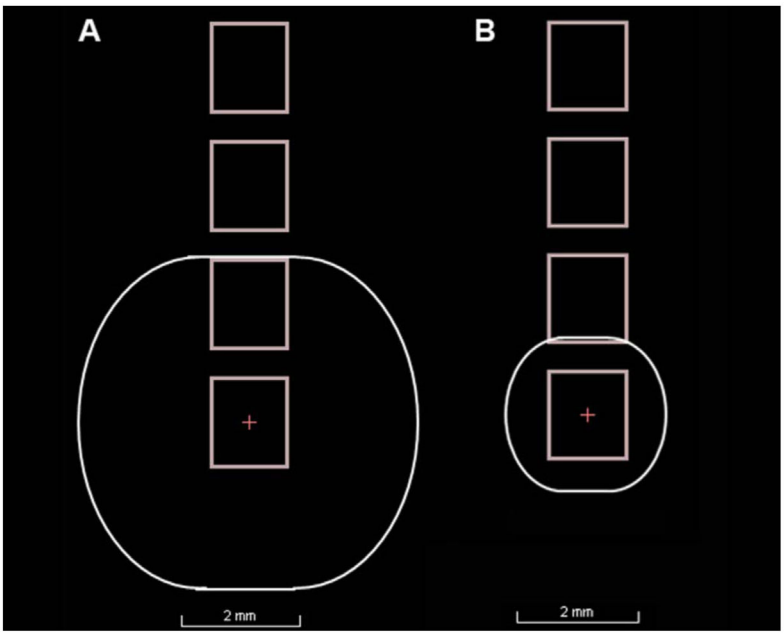

Fig. 7.

Example of the estimated VTA with average clinical stimulation settings from Experiment 1 (A) and the experimentally controlled VTA of Experiment 2 (B).

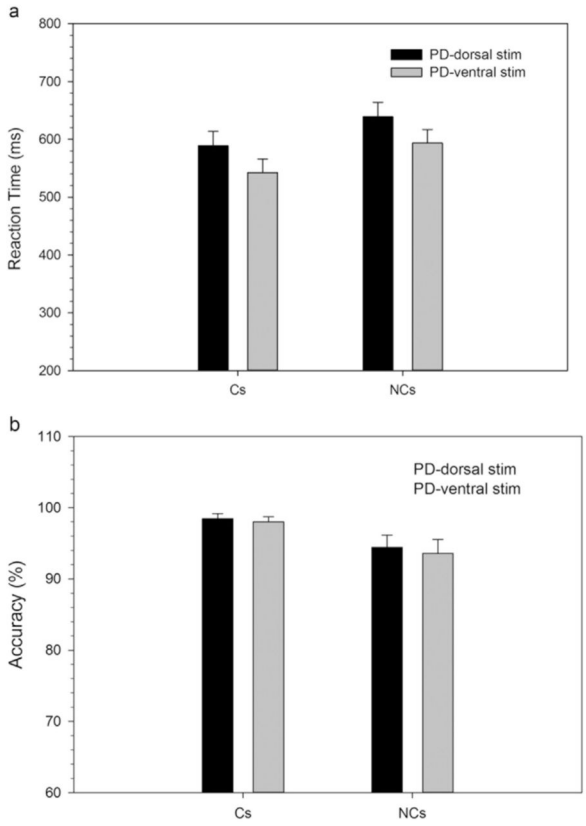

Fig. 8.

Mean RTs (A) and accuracy rates (B) on corresponding (Cs) and non-corresponding (Nc) trials types for Parkinson's disease participants on dorsal and ventral STN stimulation. Error bars reflect standard error of the means.

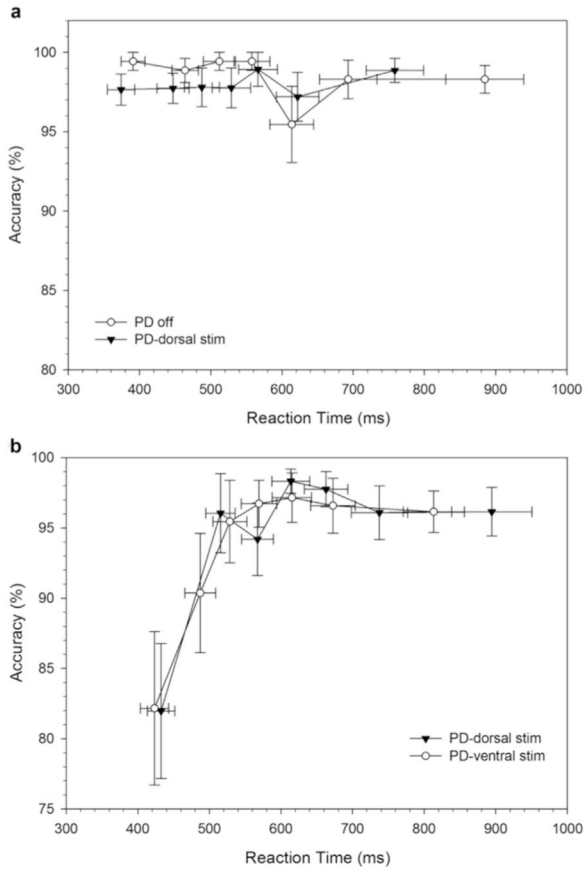

Fig. 9.

Conditional accuracy functions for corresponding (Cs, A) and non-corresponding (Nc, B) trial types for Parkinson's disease participants on dorsal and ventral STN stimulation. Errors are predominantly associated with the fastest reaction times on non-corresponding (Nc) trials, a pattern that does not vary as a function of STN subregion stimulation.

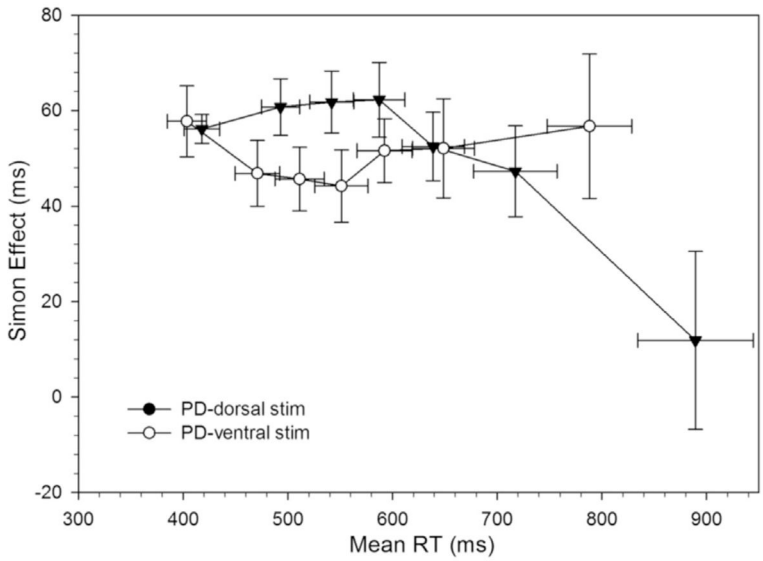

Fig. 10.

RT delta plots for Parkinson's disease (PD) participants on dorsal and ventral STN stimulation. The reduced proficiency of suppressing interference on ventral stimulation is significantly improved in with dorsal stimulation (i.e., a larger negative-going delta slope at the slow end of the distribution).

Table 1

Demographic Data (means and standard error) for the PD patients and healthy controls.

	HC (n=22)	PD exp 1 (n=12)	PD exp 2 (n=11)
Sample Size (N)	22	12	11
Age (years)	63.9(1.6)	59.3(2.9)	58.9(2.6)
Gender (M: F)**	12:10	8:4	6:5
Education (years)	14.5(.7)	13.7(.6)	13.7(.7)
MMSE	29.4(.2)	28.9 (.35)	28.6 (.4)
CESD	7	14.9 (2.5)	
BDI-II	–	9.8 (1.7)	
LEDD	–	670.9(184.9)	500.9 (127.8)
Disease Duration (years) +	–	11.8(1.8)	12.9 (1.7)
UPDRS dorsal	–	–	30.9 (2.8)
UPDRS ventral	–	–	30.1(3.4)
UPDRS chronic	–	25.0 (3.76) n=9	–
UPDRS acute	–	24.11 (3.69) n=9	–
UPDRS OFF	–	31.66 (3.99) n=9	–

MMSE=Mini Mental State Examination, CESD=Center for Epidemiologic Studies Depression Scale, BDI-II=Beck Depression Inventory II, UPDRS=Unified Parkinson's Disease Rating Scale Motor, LEDD=Levodopa Daily Dosis

Table 2

Clinical stimulation settings (means and standard error) for PD patients in experiment 1 and experiment 2.

	PD exp 1	PD exp 2
DBS Settings		
Sample Size (N)	12	11
Left		
Voltage(V)	2.3(.2)	2.6 (.3)
Frequency (Hz)	155.3(8.8)	125.5(2.8)
Pulsewidth (ms)	86.1(6.4)	59(4.8)
Right		
Voltage(V)	2.5(.3)	2.4(.3)
Frequency (Hz)	129.4(12.0)	125.5(2.8)
Pulsewidth (ms)	95.1(8.9)	61.7(5.6)

Table 3

Contacts positions included in dorsal and ventral stimulation, separate for left and right electrode. Left and right hemisphere lead positions range from 0 to 3 (ventral to dorsal).

Subject ID	Ventral contact		Dorsal contact	
	Left	Right	Left	Right
PD01	2	2	3	3
PD02	2	2	3	3
PD03	1	1	2	2
PD04	0	0	1	1
PD05	0	2	2	3
PD06	1	2	2	3
PD07	0	0	2	2
PD08	0	0	1	1
PD09	2	1	3	2
PD10	1	1	2	2
PD11	1	1	2	2